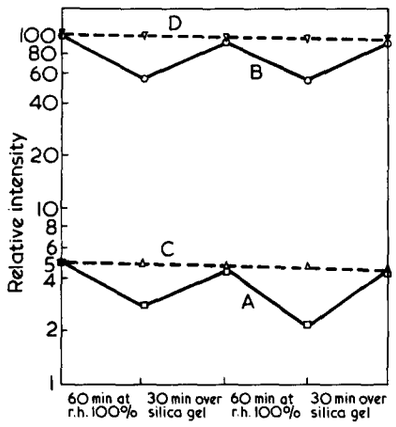

Figure 2 Variation of afterglow and phosphorescence emission intensity with exposure to high relative humidity and subsequent drying over silica gel for materials: A, undoped BL 34 Resin; B, carbazole doped BL 34 Resin; C, undoped crystalline melamine; D, carbazole doped melamine crystals. Relative intensity is indicated on a logarithmic scale

relative concentrations of carbazole and melamine are of critical importance in the solution case. In our qualitative work, only 10% of the samples produced melamine crystals having incorporated molecular carbazole. Luminescence characteristics established that the carbazole was monodispersed. Crystals obtained by both methods show phosphorescence intensities about 10 times stronger than that for the weak afterglow of the pure melamine crystals. The exposure of these crystals to high humidity and drying over silica gel did not affect the phosphorescence intensity. The normalized curve for undoped melamine crystals, see curve C of *Figure 2*, may be compared with that for the carbazole doped melamine crystals, see curve D *Figure 2*. The similarities of curves A and B along with those of curves C and D point out quite clearly that the weak and strong carbazole dopant phosphorescence intensities are only affected by water vapour in the low cured resin system. The crystalline melamine, the melamine crystallites incorporating carbazole molecules and the fully cured resin system, each are not affected by water vapour as far as the phosphorescence intensity is concerned.

The melamine phosphorescence, observed for pure crystalline melamine and for the melamine–formaldehyde resin, is not characteristic of that derived from a monodispersed system, the latter being expected to show some vibrational structure. We have, however, shown a fluorescence which we can attribute to monodispersed melamine, using PMMA as a host, and which is characteristically different from the broad, almost featureless, fluorescence of the melamine or of the commercial melamine resin. The phosphorescence observed, we believe, is due to interaction between melamine molecules, possibly of a dimeric nature (see for example ref 5). In the case of carbazole in the melamine crystalline host, the phosphorescence is suggestive of a monodispersed system, however, the strong intensity indicates that an energy transfer mechanism is available, e.g., triplet–triplet transfer from the host to the carbazole.

Considering the typical intense room temperature phosphorescence of doped thermoset melamine–formaldehyde, this is perhaps due to methylol-type free chain ends present in the low cured resin. At this stage it is not clear whether these chain ends increase the triplet–triplet energy transfer by means of the large volume of hydrogen bonded systems surrounding each carbazole dopant molecule or whether hydrogen bonding of the matrix affects the internal S_1 to T_1 transfer efficiency of the carbazole molecule. We recall, for example, that hydrogen bonding, between benzophenone and carbazole in an EPA glass at 77K, was proven to be responsible for a significant increase in benzophenone phosphorescence at the expense of carbazole phosphorescence[6].

Furthermore, phosphorescence of this system was also sensitive to the presence of hydrogen bonding matrices. This much is also clear from our results in *Figure 2* (curves A and B) which show that the presence of water vapour appears to alter the degree of hydrogen bonding, implicating the methylol chain ends and/or the similar bonding between methylolated melamine and the carbazole dopant. Our earlier studies have also indicated increased S_1 to T_1 transfer of carbazole in the thermoset resin resulting in increased phosphorescence at the expense of fluorescence, in a manner similar to the findings of Spencer and O'Donnell[6]. The matrix is not fully understood, having complex fluorescence and phosphorescence properties of its own. Nevertheless, we believe that its role as a donor species is proven beyond doubt.

We are in the process of making melamine–formaldehyde resins with differing numbers of methylol groupings (lowest 1 to highest 6) in order to elucidate the role of the methylol groupings in the strong room temperature phosphorescence of this system and possibly clarify the mechanism by which water vapour affects the phosphorescence reversibly.

Acknowledgement

We thank the ILEA for a research assistantship to one of us (N. H.).

D. J. Morantz, C. S. Bilen and N. Harrison

London College of Printing, Elephant and Castle, London SE1, UK

(Received 2 December 1977)

References

1 Morantz, D. J., Bilen, C. S. and Thompson, R. C. in 'Reactivity of Solids,' (Eds J. Wood, O. Lindqvist, C. Helgesson and N. -G. Vannerberg), Plenum Press, New York and London, 1977, p 499
2 Bilen, C. S. and Morantz, D. J. *Polymer* 1976, **17**, 1091
3 Wohnseidler, H. P. *Ind. Eng. Chem.* 1953, **45**, 2307
4 Morantz, D. J., Bilen, C. S. and Harrison, N. *Int. Conf. Radiationless Processes Breukelen, The Netherlands, August 1977* p 81
5 Bilen, C. S., Harrison, N. and Morantz, D. J. *Nature* 1978, **271**, 235
6 Spencer, T. S. and O'Donnell, C. M. *J. Am. Chem. Soc.* 1972, **94**, 4846

On the possibility of crankshaft motion in polymers in dilute solution

Introduction

The local mode explanation of the molecular weight independent high frequency relaxation process in dilute polymer solutions requires the concept of a localized segmental motion which leaves the bulk of the molecule completely undisturbed. The most likely mechanism for this process is the crankshaft model proposed by Schatzki[1], in which five carbon–carbon bonds (numbered 2 to 6 in *Figure 1*) consti-

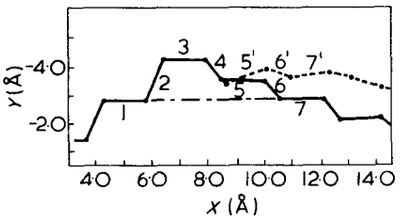

Figure 1 A projection onto the $X-Y$ plane of the initial position of the crankshaft both before relaxation of the rotational angles (———), and after relaxation (– – –)

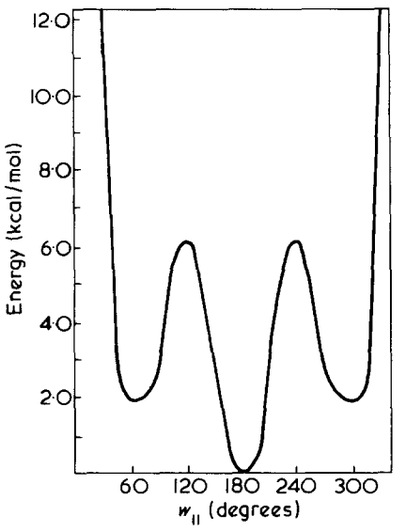

Figure 2 The minimum energy path for rotation of the crankshaft

tute the crankshaft, and additional bonds at either end (1 and 7) provide the 'stem' about which the crankshaft rotates.

An essential criterion for this model is that bonds 1 and 7 remain colinear, and provided that the internal rotation angles about the carbon–carbon bonds can only occupy the three traditional states of *trans, gauche* plus and *gauche* minus (denoted by T, G^+ and G^-, respectively), then a TG^+TG^+T sequence of the five internal bonds results in exact colinearity of the stems, and the crankshaft is free to rotate to any of its three equilibrium positions, while at the same time leaving the remainder of the molecule completely motionless.

An underlying assumption here is that the isomeric three state model provides a valid description of internal rotation in polyethylene molecules. It has come to be accepted however that this is not true, and in fact the calculations of Scott and Sheraga[2] show quite clearly that in a given sequence of T, G^+ and G^- bonds significant departures (by as much as 20°) of the rotational angles from their traditional equilibrium values can occur. The introduction of these states into a Schatzki crankshaft destroys the colinearity of the stems and raises the question of whether or not the crankshaft model can still provide a plausible description of the local mode process.

In this Letter we use the method of Scott and Scheraga to calculate the minimum energy path for rotation of a Schatzki crankshaft in $C_{15}H_{32}$. By using an energy minimization on each dihedral angle of internal rotation, rather than just assuming the simple isomeric three state model, we find that as the crankshaft rotates the end of the molecule undergoes such a large displacement that the localized nature of the motion is completely lost.

Computer calculations

The conformational energy was calculated using the method outlined in the paper by Scott and Scheraga. As their description is a particularly clear one we will only briefly describe the method here, and the interested reader is referred to the original paper for more details. There are two contributions to the energy, an exchange interaction of electrons in bonds adjacent to the bond about which internal rotation occurs, and non-bonded interactions between all the pairs of atoms not covalently bonded to each other. The exchange interaction depends on both the dihedral angles of internal rotation, which are free to assume any value, as well as on all the fixed bond angles, which in this case were set equal to their experimentally determined values. The non-bonded interactions were calculated via a Lennard-Jones '6–12' potential, the coordinates of all the atoms first being transferred to a frame of reference centered on the first hydrogen atom via a matrix multiplication. This also enabled us to keep track of the position of each atom as the crankshaft rotated. The interaction parameters for the '6–12' potential were taken from Scott and Sheraga's paper.

Because we are more interested in the motion of the molecule as the crankshaft rotates, rather than exact values for the energy barriers, our minimization procedure is less involved than that of Scott and Sheraga. We begin with the 5 internal crankshaft bonds in the TG^+TG^+T configuration (our convention here is that the T state occurs at 180°, G^+ at 60° and G^- at 300°), all other bonds being in the *trans* state. This represents the 'ideal' crankshaft conformation. Starting at the first C–C bond we then vary the rotational angle w_1 by a fixed amount Δ (5° in this calculation), while at the same time keeping all other rotational angles constant. The direction of the change is chosen so that the total conformational energy of the molecule is lowered. If we find that the energy cannot be lowered by a change in either direction then we are clearly already at the bottom of a potential well and the angle is left unaltered. We continue in this way along the length of the chain, successively minimizing each dihedral angle (except for the two angles w_5 and w_{11}, about which the rotation occurs) until we come to the end of the chain. We then compare the energy with the value computed at the start of the minimization and repeat the process until the two energies are the same, which will occur when each dihedral angle is at its lowest energy position. We then record the position of each carbon atom, the crankshaft is rotated through 30°, and the entire process is repeated until the crankshaft has rotated through a full 360°.

The molecule used in our calculations was the straight chain hydrocarbon $C_{15}H_{32}$. The bond lengths and bond angles were representative values taken from the paper of Scott and Sheraga, i.e. 1.533 Å for the C–C bonds and 1.120 Å for the C–H bonds. The bond angles were 112.7° for the CCC angles, 110.5° for the CCH angles, and 108.4° for the HCH angles.

Discussion

The result of allowing the dihedral angles to relax into their minimum

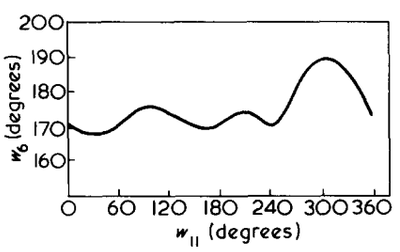

Figure 3 Variation of the first internal rotational angle in the crankshaft as the minimum energy path is traversed. If the isomeric three state scheme applied this angle would remain constant at 180°

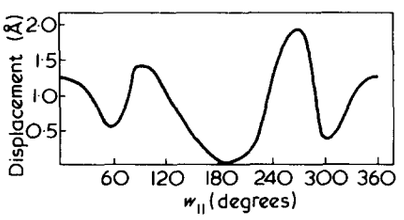

Figure 4 Displacement of the end of the crankshaft as rotation occurs

energy configuration is shown in *Figure 1*. The full line shows the position of the crankshaft in the 'ideal' (i.e. isomeric state) configuration and the broken line shows its position after the dihedral angles have relaxed. We can see quite clearly that the stems are no longer colinear, so that rotation of the crankshaft will produce a disturbance in the rest of the molecule, and that several of the angles are severely distorted from their isomeric state values, e.g. the *trans* bond in the middle of the crankshaft is now at 160° rather than 180°.

The minimum energy path for the rotation of this crankshaft is shown in *Figure 2*. The curve has the expected triple well shape, and the height of the barriers was found to be quite accurately approximated by the sum of the individual barriers encountered by each 'stem' bond rotating separately. *Figure 3* shows the variation in w_6, the first dihedral angle in the crankshaft, with the angle of rotation. Contrary to the hopes of Schatzki, and the calculation of Boyd and Breitling[3], we find that there is quite a variation in the values of all the crankshaft bonds as rotation occurs. The 20° variation illustrated in *Figure 3* is quite characteristic of the behaviour of each of the bonds adjacent to a 'stem' bond.

The effect of this variation in angle and non-colinearity of the stems can be seen in *Figure 4*, where we plot the position of C_{10} which is the carbon atom at the 'fixed' end of the crankshaft, as a function of rotational angle. Distance is measured from the initial relaxed position before the start of rotation. For an ideal crankshaft this particular atom should of course remain motionless, whereas *Figure 4* shows that as the crankshaft passes through the eclipsed position at 270° the carbon atom has been displaced from its equilibrium position by almost 2 Å. This is quite a large displacement when compared to the length of the crankshaft, which is only about 5 Å, and for atoms further down the chain this effect is magnified rather than reduced, the end carbon atom, for example, being displaced from its equilibrium position by as much as 6 Å.

The most appealing aspect of the crankshaft model, when considered in the frame of the rotational isomeric three state scheme, is the completely localized nature of the motion. However our calculations show that when allowance is made for more realistic equilibrium rotational angles this localized nature is lost, and that a crankshaft endeavouring to rotate from one equilibrium state to another through the lowest energy path would involve considerable movement of the remainder of the polymer molecule. Whether or not the solvent molecules would allow this type of motion is uncertain, nevertheless, we feel that the results described here cast serious doubt on the ability of the crankshaft mechanism to provide a useful description of the local mode process in dilute polymer solutions.

Acknowledgements

The authors are indebted to Dr R. A. Pethrick for providing assistance with the computer programme, and to the Science Research Council for financial support of the programme concerning molecular motion in polymers currently under study at Strathclyde University.

D. A. Jones and D. Pugh

Department of Pure and Applied Chemistry, University of Strathclyde, Glasgow G1 1XL, UK

(Received 28 November 1977)

References

1 Schatzki, T. F. *Polym. Prepr.* 1965, 6, 646
2 Scott, R. A. and Scheraga, H. A. *J. Chem. Phys.* 1966, **44**, 3054
3 Boyd, R. H. and Breitling, S. M. *Macromolecules* 1974, 7, 855

Effect of hydrogenation on the elastic properties of poly(styrene-*b*-diene-*b*-styrene) copolymers

Introduction

Teleblock copolymers poly(styrene-*b*-butadiene-*b*-styrene) and poly(styrene-*b*-isoprene-*b*-styrene), widely used for their elastoplastic properties, suffer severe drawbacks in their application due to poor ageing properties of the unsaturated soft phase, poor long term elastic properties (stress relaxation as measured by compression set) at temperatures as low as 20°–30°C, short term elastic properties (instantaneous recoverable deformation as measured by tension set) and rapidly decreasing tensile properties as a function of temperature.

In principle, these properties could be improved by introducing saturated soft phases and hard phases with higher glass transitions or melting points. This can be easily carried out by means of hydrogenation: the soft phase becomes a saturated rubber and the hard phase a polyvinylcyclohexane resin with a glass transition nearly 50°C higher than that of polystyrene. While the effect of the hydrogenation of the soft phase on the ageing properties is well known, no data were reported in the literature, as far as we know, on the effect of hydrogenation of both soft and hard phases on the elastic properties.

Experimental

Samples. Hydrogenation was carried out on two commercial teleblock copolymers, a poly(styrene-*b*-isoprene-*b*-styrene) (SIS) and a poly(styrene-*b*-hydrogenated high vinyl butadiene-*b*-styrene) (SEBS) with the following characteristics:

	Styrene (wt %)	M_n (osm)
SIS	17	88.200
SEBS	30	58.000

Hydrogenated SIS may be considered as a (VCH–EP–VCH) copolymer and hydrogenated SEBS as (VCH–EB–VCH) copolymer, where VCH indicates a polyvinylcyclohexane block, EP an alternate ethylene–propylene copolymer and EB an ethylene–butene-1 copolymer obtained by hydrogenation of high vinyl polybutadiene.

Hydrogenation was carried out at